pp. 1–13 (2023)

Myocardial perfusion segmentation and partitioning methods in personalized models of coronary blood flow

A. A. Danilov[abcd], T. M. Gamilov[abde], F. Liang[f], A. A. Rebrova[b], P. Sh. Chomakhidze[e], Ph. Yu. Kopylov[e], Y. R. Bravyy[d], and S. S. Simakov[abc]

Abstract — In this work we present methods and algorithms for construction of a personalized model of coronary haemodynamics based on computed tomography images. This model provides estimations of fractional flow reserve, coronary flow reserve, and instantaneous wave-free ratio taking into account transmural perfusion ratio indices obtained from perfusion images. The presented pipeline consists of the following steps: aorta segmentation, left ventricle wall segmentation, coronary arteries segmentation, construction of 1D network of vessels, partitioning of left ventricle wall, and personalization of the model parameters. We focus on a new technique, which generates specific perfusion zones and computes transmural perfusion ratio according to the quality of available medical images with a limited number of visible terminal coronary vessels. Numerical experiments show that accurate evaluation of stenosis before precutaneous coronary intervention should take into account both fractional flow reserve indices and myocardial perfusion, as well as other indices, in order to avoid misdiagnosis. The presented model provides better understanding of the background of clinical recommendations for possible surgical treatment of a stenosed coronary artery.

Keywords: Medical image segmentation, coronary circulation, myocardial perfusion, transmural perfusion ratio, fractional flow reserve, coronary flow reserve, instantaneous wave-free ratio

MSC 2010: 92C55, 65D18, 68U10, 37M05, 92B99

Coronary artery disease (CAD) is the leading cause of mortality worldwide. Stenosis of coronary arteries is one of the common causes of decreased coronary blood flow leading to myocardial ischemia. In severe cases of CAD, the precutaneous coronary intervention (PCI) procedure is used to treat the coronary arteries stenosis. Fractional flow reserve (FFR) is a golden standard for assessing the haemodynamic significance of the stenosis [9, 18]. The other useful indices are instantaneous wave-free ratio (iFR) and coronary flow reserve (CFR) [9, 10]. They require direct invasive

[a]Marchuk Institute of Numerical Mathematics of the RAS, Moscow 119333
[b]Moscow Institute of Physics and Technology, Dolgoprudny 141701
E-mail: simakov.ss@phystech.edu
[c]Sechenov University, Moscow 119435
[d]Sirius University of Science and Technology, Sochi 354340
[e]World-Class Research Center 'Digital biodesign and personalized healthcare', I. M. Sechenov First Moscow State Medical University (Sechenov University), Moscow 119991
[f]Shanghai Jiao Tong University, Shanghai 200240, China
The research was supported by the joint RSF-NSFC project (Russian Science Foundation, grant No. 21-41-00029 and National Natural Science Foundation of China, grant No. 12061131015).

measurements of the intra-vessel pressures or flows. The non-invasive alternatives are more preferable for estimation of the FFR values, e.g., virtual fractional flow reserve (vFFR) or Computed Tomography Fractional Flow Reserve (CT-FFR, FFR-CT) [14, 17, 26]. The virtual FFR, iFR, and CFR values are calculated from personalized models of coronary blood circulation based on computed tomography (CT) images [21]. The work [12] presents a reduced order method approach aggregating eleven physiological and anatomical factors to a real time evaluation of FFR. The work [25] presents a recent review of modern mathematical models of coronary blood flow.

Another common cause of CAD is impaired microcirculation of the myocardium, which may be also observed without any substantial coronary stenoses. Recent studies showed that coronary microcirculation dysfunction is a predictive factor for residual myocardial ischemia, which remains in numerous patients even after PCI treatment [1]. In order to improve clinical accuracy of pre-operative diagnostics, recent studies investigate various perfusion indices [20] and their combination with FFR and other haemodynamic indices [2, 13]. Modern mathematical models of coronary haemodynamics tend to adopt the use of CT perfusion data (CTP) for CAD evaluation [8, 15].

In our previous work, we showed that microvascular perfusion impairment plays significant role in correct computational estimation of haemodynamic indices before PCI [22]. The peripheral hydraulic resistance of myocardial perfusion is personalized based on transmural perfusion ratios of standard zones [22] and individual zones [23]. The biomechanical model of coronary haemodynamics was lately improved with 0D lumped parameter boundary conditions [24]. The personalized model is incorporated into a new web-based computational technology for non-invasive estimation of FFR from patient CT data [27].

The main problem of the previous approach [22] is insufficient quality of CT scans. Low resolution of CT scans reduces the number of visible arteries. We typically observe less than 10 terminal arteries. A correct model must connect every perfusion zone to at least one feeding artery. The standard CTP protocol provides decomposition into 32 zones. The main novelty of this work is adjustment of the number of perfusion zones to visible terminal vessels of the coronary tree after segmentation of CT scans.

In the present work, we demonstrate details of methods and algorithms for construction of a personalized coronary flow model and virtual assessment of FFR, iFR, and CFR for patients with reduced myocardial perfusion. The model includes additional terminal conditions, which depend on the perfusion indices. In order to compute these indices, we partition the myocardium of the left ventricle into generic zones corresponding to the coronary tree segments. We assume that every terminal coronary artery supplies one generic zone of myocardium. Next, we compute the average transmural perfusion ratio across the zone, and attach it to the terminal segments of the coronary tree. All steps are performed in automatic or user-guided way to speed up the simulation. The presented model provides a better understanding of the background of PCI recommendations based on FFR, iFR, and CFR.

The paper is organized as follows. In Section 1 we present the pipeline, algorithms and methods for image processing and mathematical modelling. In Section 2 we demonstrate an application of our methodology to the clinical practice. In Section 3 we discuss the results.

1. Main algorithm

The mathematical model of the coronary flow is based on a 1D network of the coronary vessels reconstructed from the patient CT image. Coronary CT angiography (CTA) is usually the preferred choice for detailed reconstruction of coronary vessel structure and especially for detecting stenotic regions. At the same time, the myocardial CT perfusion (CTP) imaging provides both anatomical and functional evaluation of the coronary blood flow, allowing one to both reconstruct the anatomical structure of the coronary network and estimate the myocardial perfusion dysfunction. CTP images may be used solely as a universal data source for constructing personalized models of coronary blood flow. Alternatively, CTA image may be used to construct the coronary network, and CTP image may be used to estimate perfusion. In the latter case, an additional step may be required to align the images if they were captured at different times. In the current work, we assume that the sole CTP image is used for simplicity.

Once the CT image is obtained, the personalized model may be constructed in the following steps:

1. Image preprocessing;
2. Aorta segmentation;
3. Left ventricle wall segmentation;
4. Coronary arteries segmentation and construction of 1D network of vessels;
5. Partitioning of left ventricle wall;
6. Personalization of the model parameters.

Some of these steps were presented in detail in our previous works [27, 4, 28]. We discuss them briefly in this work, giving more details to the new Steps 3 and 5.

During the preprocessing step (Step 1) the CT image is cropped to include both left and right ventricles and cut the ascending aorta between the aortic valve and the aortic arch (Fig. 1). This step is needed to improve the detection of aorta on the CT image and to reduce the computational costs of the following segmentation algorithms. If the voxel size is highly anisotropic, then additional resampling is preferable to make voxel sizes more isotropic, i.e., close to the cubic shape.

At Step 2 the aorta is segmented in four major phases (Fig. 2). First, the aorta is detected on the topmost slice as the largest bright disk using circle Hough transform [6] (Fig. 2a). Second, the average image intensity inside the disk is used as

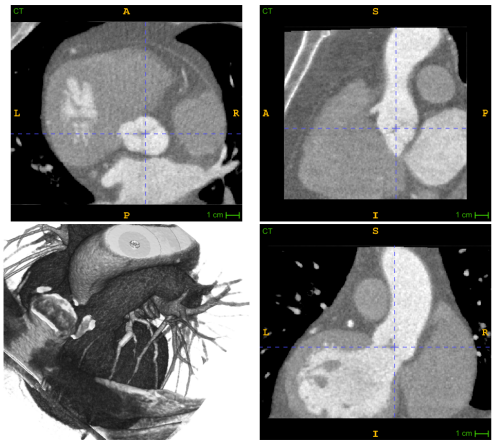

Figure 1. Cropped CTP image showing high contrast in ventricles, moderate intensities in myocardial wall, and low intensity in the surrounding tissues.

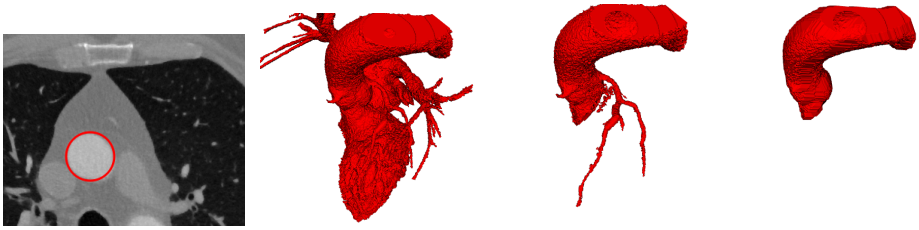

(a) (b) (c) (d)

Figure 2. Aorta segmentation steps: (a) largest disk detected by circle Hough transform, (b) threshold-based segmentation, (c) aorta segmentation using Isoperimetric Distance Trees approach, (d) smoothed segmentation of aorta.

the threshold parameter and the connected region with the seed point in the center of the disk is extracted as the initial guess (Fig. 2b). Third, this guess is updated using the Isoperimetric Distance Trees (IDT) approach [4, 11] (Fig. 2c). Finally, the segmented mask of aorta is smoothed using mathematical morphology operations [28] (Fig. 2d).

At Step 3 the myocardial wall is segmented by a threshold-based method. The average intensity of myocardial wall voxels in CTP images commonly lies in the range $[80; 140]$ HU. The left ventricle wall is located around the left ventricle cavity, which has higher intensity values due to contrast enhancement. The ventricle wall can be separated from the atria by the plane passing through the mitral valve. There is a sharp change in intensity at the boundaries of the ventricle, so we focus on detecting these boundaries during segmentation. At the first stage we zero all very small, negative and very large intensities. Thus, effects of possible intensity emissions are excluded. In addition, the intensity values at the borders of the left ventricle should be positive. The volume of the left ventricle wall is extracted as a connected region clipped by the plane passing through the mitral valve (see Fig. 3). The location of the mitral plane is estimated as the plane orthogonal to the left vent-

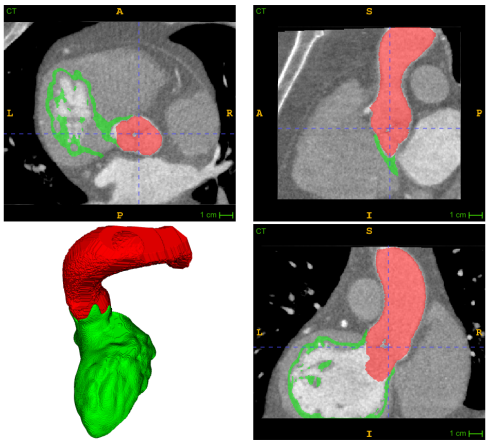

Figure 3. Segmentation of aorta and left ventricle walls for CTP image: aorta in red colour, left ventricle walls in green colour.

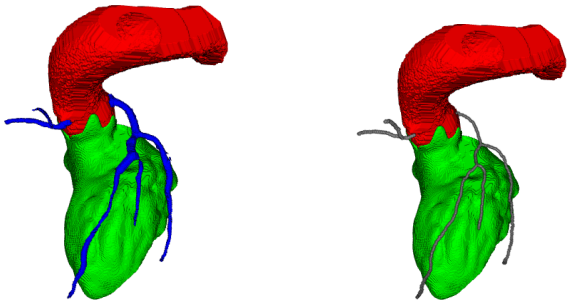

(a) (b)

Figure 4. Coronary arteries segmentation steps: (a) coronary arteries segmentation using Frangi vesselness filter, (b) centerlines of the coronary tree computed by distance-ordered homotopic thinning method, aorta in red colour, left ventricle walls in green colour, coronary arteries in blue colour, centerlines in black colour.

ricle axis and passing through the interface between the left atrium and left ventricle cavities. The user can manually override the location of the plane if necessary.

At Step 4 the coronary arteries are segmented by Frangi vesselness filter [5], the starting seeds are detected as the two voxels with the highest vesselness values on the surface of the aorta (Fig. 4a). Then, the distance-ordered homotopic thinning method [19] is used to construct the centerlines of the coronary tree (Fig. 4b). Finally, the coronary tree is partitioned to the vessel segments resulting in 1D coronary network suitable for computations [4, 28].

Detection of a myocardial perfusion defect may indicate the presence of ischemia. To assess perfusion, the transmural perfusion ratio (TPR) can be used, which is defined as the ratio of the attenuation density of the contrast agent in a segment of the subendocardium (inner layer) to the attenuation density of the contrast agent in

the entire subepicardial layer (outer layer) [3]:

$$\mathrm{TPR}_s = \frac{\mathrm{AD}_s}{\mathrm{AD}_{\mathrm{epi}}} \tag{1.1}$$

where AD_s is the attenuation density of a subendocardial segment s, and $\mathrm{AD}_{\mathrm{epi}}$ is the attenuation density of the entire subepicardial layer. The values of AD_s and $\mathrm{AD}_{\mathrm{epi}}$ are provided by CTP device for every voxel of the CTP image and for 32 standard perfusion zones.

Local TPR values may be computed in each voxel of the left ventricle wall. Once the wall is split into outer and inner parts of the wall, we calculate the average intensity value on the outer wall of the ventricle and divide the intensity of each voxel of the inner wall of the ventricle by the average intensity in the outer part. These local TPR values are used to calculate the TPR value for a certain zone as the average value of TPR values in the zone.

TPR calculations may be performed in two ways. Either the original TPR values are used during calculations, or the TPR values are clipped to the range $[0.2, 1]$, i.e., all values less than 0.2 are replaced by 0.2, and all values greater than 1 are replaced by 1. These restrictions are introduced in order to decrease the effect of local TPR disturbances.

At Step 5 the ventricle wall is partitioned into individualized zones corresponding to the segments of the 1D coronary network. The coronary tree is processed recursively starting at the virtual root uniting both left and right coronary branches. At each branching point we split the ventricle wall into several zones and proceed to the descending branching points. Finally the whole myocardial wall is split into individual zones corresponding to the terminal nodes of the coronary tree.

The partitioning of the wall is constructed depending on the distance to the coronary arteries. When the coronary artery branches for the first time, we divide it into two parts. Next, for each ventricular voxel, we calculate the distance to each of the segments of the coronary arteries. Then, we construct several zones, in each of which the distance to a certain branch is less than the distance to other branches and assign the voxel to the segment with minimal distance (see Fig. 5). Next, we take one of the branches under consideration and divide the coronary branch into segments in the same way at the branching point. Similarly, we divide the zone that belongs to this branch into individual parts (see Fig. 6). Thus, the division of the ventricle into individual zones is constructed depending on the segments of the coronary arteries.

We descend recursively through the coronary tree, splitting the myocardial wall into individual zones, corresponding to the coronary segments. During this process we advance to a next branching point, we take only the part of the ventricle that already belongs to the parent branch, and divide it into parts in the same way. Once all branching points are processed, we end up with the partitioned myocardial wall corresponding to the terminal segments of the coronary tree (see Fig. 7).

Finally, at Step 6 the TPR values of individual zones are computed as the average TPR values. As discussed above, the clipping of the TPR values may be used before

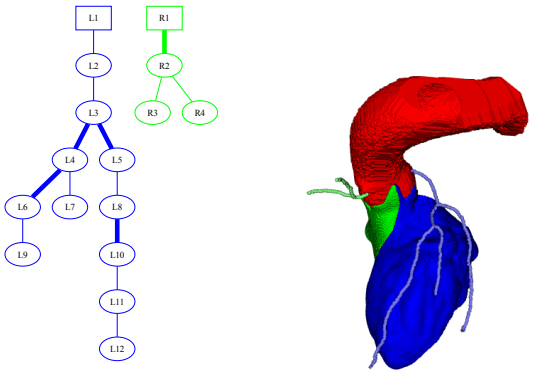

Figure 5. Partitioning of the left ventricle wall into two parts, corresponding to the left (L1, blue) and right (R1, green) coronary arteries, aorta is shown in red.

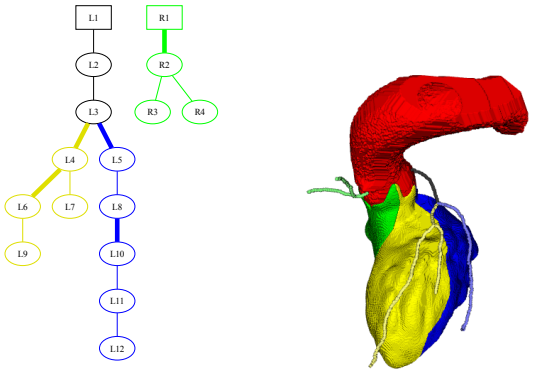

Figure 6. Partitioning of the left ventricle wall into three parts, corresponding to the left anterior descending artery (L4, yellow), left circumflex artery (L5, blue) and right coronary artery (R1, green), aorta is shown in red.

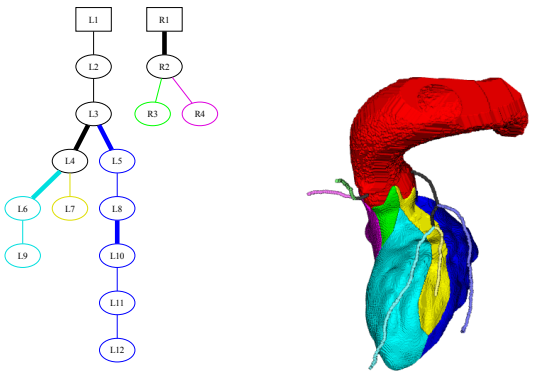

Figure 7. Final partitioning of the left ventricle wall, aorta is shown in red.

averaging in order to reduce the disturbance of local TPR values.

Areas with TPR values above 1.0 are considered to be healthy. Values between 0.94 and 1.0 demonstrate mild perfusion disorder. Values below 0.94 are associated with severe perfusion disorder. These perfusion indices may be included in the mathematical model as an additional multiplier for the hydraulic resistance as proposed in our previous work [23]. The multiplier is equal to one for all zones with TPR above 1.0. As TPR value descends towards 0.94, the multiplier increases gradually. Once the TPR value drops below 0.94, the multiplier increases rapidly.

The proposed pipeline was developed as a standalone C++ code, which extensively uses ITK library [16] for basic image operations.

2. An example of clinical usage

In this section we present an example of haemodynamic simulations that utilize presented algorithm. The coronary blood flow model was described in detail in [21, 22, 23]. Blood flow in the coronary arteries and the aorta is simulated as 1D axisymmetric flow of Newtonian viscous incompressible fluid through the network of elastic tubes. The structure of the coronary network is extracted from CT images (see Steps 2 and 4 above). On the inlet of the network we set cardiac output as the boundary condition. On the outlets of peripheral coronary arteries we set hydraulic resistances to simulate the myocardial perfusion. The peripheral hydraulic resistance of the myocardial perfusion is personalized based on patient TPR data and position of coronary arteries. Lower TPR (TPR < 1.0) values increase peripheral resistances to simulate impaired perfusion.

The goal of simulations with the model of coronary blood flow is to compute pressure and flow in coronary arteries as functions of space and time. After that, we calculate a set of haemodynamic indices for each stenosis. We compute them according to the following definitions.

- Fractional Flow Reserve (FFR) is the ratio of the mean pressure in a coronary artery distal to a stenosis and the mean aortic blood pressure during hyperemia. FFR ranges between 0 and 1. The values of FFR between 1.0 and 0.8 correspond to insignificant stenosis. The values less than 0.8 are considered as possible indication for PCI.

- Instantaneous wave-free ratio (iFR) is the ratio between the mean pressure in a coronary artery distal to a stenosis and the mean aortic blood pressure during the diastolic wave-free period. iFR ranges between 0 and 1. The value 1.0 corresponds to an insignificant stenosis. The values less than 0.9 are considered as possible indication for PCI.

- Coronary flow reserve (CFR) is the ratio of the mean blood flow through a stenosed vessel during hyperemia to the mean blood flow through the stenosed vessel under normal conditions. CFR typically ranges between 1.0 and 4.0. The values greater than 3.0 correspond to a healthy vessel. The values below 2.0 are considered as possible indication for PCI.

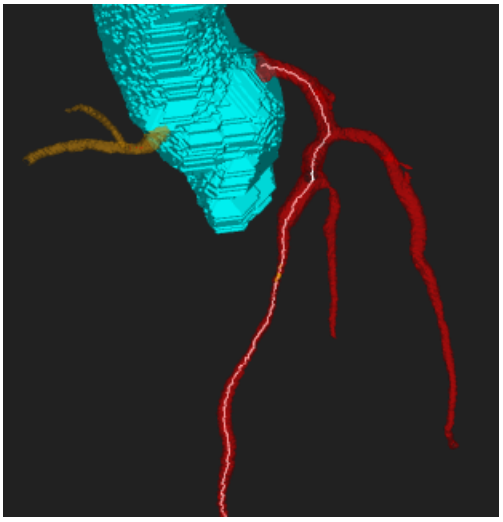

Figure 8. Segmented structure of left(red) and right(orange) coronary arteries of a patient. White line designates left anterior descending artery.

We calculate FFR, CFR, and iFR in three cases: before the treatment, immediately after the treatment, and 3 months after the PCI. We collect CT images and TPR values before PCI and use them for calculating the indices before the treatment and immediately after the treatment. In the second case we substitute occluded region with a healthy lumen. We assume that a possible microcirculation impairment can not be recovered by increasing pressure in a short period and thus we use the same TPR values. We use CT images and TPR values after PCI to calculate indices 3 months after the treatment. They give us data on changes of vascular lumens and the state of microcirculatory regions.

We process anonymous retrospective data from a patient of the Clinical center of Sechenov University. The patient suffered from a chest pain and angina. CT images showed a stenosis in the left anterior descending artery (LAD). The segmented structure of patient's coronary arteries is presented in Fig. 8. The white line represents LAD with a 90% stenosis in the middle part. The TPR values for myocardium regions supplied by LAD are between 0.89 and 0.93. Invasively measured FFR for this stenosis is 0.81, which is an unexpectedly high value for a 90% stenosis and TPR < 0.95. The FFR value does not designate stenosis as haemodynamically significant, but the TPR values show impaired perfusion. A stent was placed in LAD to treat the stenosis and a second set of CT images was obtained 3 months after the treatment.

We summarize the results of numerical simulations in Tables 1 and 2. Table 1 shows haemodynamic indices calculated with the help of TPR values of myocardium regions. In the first case, the calculated FFR value (0.8) is very close to the measured one (0.81). The iFR and CFR values were not measured. The FFR value formally classifies the stenosis as insignificant, the iFR and CFR values classify the stenosis as significant (iFR < 0.9, CFR < 3.0).

Table 2 shows haemodynamic indices calculated regardless the status of the perfusion (all TPR values were set to 1.0). In this case, the FFR, iFR, and CFR

Table 1. Calculated indices of a stenosis in LAD before and after the treatment using information on a myocardium perfusion.

Period	FFR	iFR	CFR
Before PCI	0.8	0.81	2.18
After PCI	0.99	0.99	2.61
Long-term	0.98	0.99	3.07

Table 2. Calculated indices of a stenosis in LAD before and after the treatment ignoring information on a myocardium perfusion.

Period	FFR	iFR	CFR
Before PCI	0.77	0.8	2.32
After PCI	0.99	0.99	2.89
Long-term	0.98	0.99	3.07

values classify stenosis as significant even though CFR in the second case is greater, than in the first one.

We observe a significant difference in the computed values of FFR and CFR before PCI in the first and second cases. We see excellent values of FFR and iFR immediately after the treatment in both cases. We also observe intermediate values of CFR in both cases, although the second approach provides more optimistic evaluation. Both models produce the same values of the indices in long-term, which can be interpreted as a possibly successful recovery.

We note that the second method provides better prognosis in favour of actual clinical decision, but the error of FFR evaluation (5%) is larger than that in the first case (1%). It is interesting that both invasively measured and accurately simulated FFR do not require PCI treatment. However, the stenosis was treated and CFR values reached a healthy threshold. The reason is as follows. The low value of TPR downstream the stenosis indicates to a region with impaired perfusion and increased terminal resistance. As a result, excessive amount of blood is accumulated downstream the stenosis, particularly during hyperemia. It inflates the artery and increases the pressure after the stenosis. Thus, formally FFR value increases and FFR-based decision may incorrectly classify stenosis as insignificant. Therefore, FFR must be accurately analyzed together with myocardial perfusion and other indices (iFR, CFR).

3. Discussion and conclusions

The presented algorithms allow us to refine the pipeline for CT image processing and personalization of the mathematical model of coronary blood flow. Some of the presented steps were implemented in a user-friendly web-based interface for non-invasive estimation of vFFR [27]. Our recent research shows that myocardial perfusion defects may affect the results of computations [22]. Thus, an automated segmentation and partitioning of the perfusion images play the vital role in improvement of model accuracy [23]. The main novelty of this work is the additional model personalization via the new CTP-segmentation technique for generation of limited number of the perfusion zones adjusted to visible terminal vessels.

Although the segmentation algorithms were designed to be fully automatic, we

still rely on interaction with the user. In most cases default segmentation parameters are sufficient to construct a 1D model of the coronary network. However, locations of stenoses and their severity should be controlled by the user. This final step should be also automated in the future.

Better understanding of contrast matter propagation through the myocardium tissue may improve the TPR evaluation technique and increase accuracy of the model. The multilayer model of the myocardium [7] may be a useful tool for that. Although the proposed pipeline needs further extensive evaluation, our first results show that evaluation of a stenosis before PCI should take into account both fractional flow reserve values and myocardial perfusion, as well as other indices, to avoid misdiagnosis.

Acknowledgement: We acknowledge the help of Daria Gognieva, Mariam Gappoeva and other involved staff of Sechenov University in collecting medical data.

References

1. S. Aggarwal, F. Xie, R. High, G. Pavlides, and T. R. Porter, Prevalence and predictive value of microvascular flow abnormalities after successful contemporary percutaneous coronary intervention in acute ST-segment elevation myocardial infarction. *J. Amer. Soc. Echocardiog.* **31** (2018), No.!6, 674–682.
2. A. Coenen, A. Rossi, M. M. Lubbers, A. Kurata, A. K. Kono, R. G. Chelu, S. Segreto, M. L. Dijkshoorn, A. Wragg, R.-J. M. van Geuns, F. Pugliese, and K. Nieman, Integrating CT myocardial perfusion and CT-FFR in the work-up of coronary artery disease. *JACC: Cardiovascular Imaging* **10** (2017), No. 7, 760–770.
3. E. Contea, FFRCT and CT perfusion: A review on the evaluation of functional impact of coronary artery stenosis by cardiac CT. *Int. J. Cardiol.* **300** (2020), 289–296.
4. A. Danilov, Y. Ivanov, R. Pryamonosov, and Y. Vassilevski, Methods of graph network reconstruction in personalized medicine. *Int. J. Numer. Methods Biomed. Eng.* **32** (2015). No. 8, e02754.
5. A. F. Frangi, W. J. Niessen, K. L. Vincken, and M. A. Viergever, Multiscale vessel enhancement filtering. In: *Medical Image Computing and Computer-Assisted Intervention — MICCAI'98*. Springer, Berlin–Heidelberg, 1998, pp. 130–137.
6. R. O. Duda and P. E. Hart, Use of the Hough transformation to detect lines and curves in pictures. *Commun. ACM* **15** (1972), No. 1, 11–15.
7. X. Ge, Z. Yin, Y. Fan, Y. Vassilevski, and L. Fuyou, A multi-scale model of the coronary circulation applied to investigate transmural myocardial flow. *Int. J. Numer. Methods Biomed. Eng.* **4** (2018), e3123.
8. X. Ge, Y. Liu, S. Tu, S. Simakov, Y. Vassilevski, and F. Liang, Model-based analysis of the sensitivities and diagnostic implications of FFR and CFR under various pathological conditions. *Int. J. Numer. Methods Biomed. Eng.* **37** (2019), No. 11.
9. M. Götberg, E. Christiansen, I. Gudmundsdottir, L. Sandhall, M. Danielewicz, L. Jakobsen, S. Olsson, P. Öhagen, H. Olsson, E. Omerovic, F. Calais, P. Lindroos, M. Maeng, T. Tödt, D. Venetsanos, S. James, A. Karegren, N. M., J. Carlsson, D. Hauer, J. Jensen, A. Karlsson, G. Panayi, D. Erlinge, and O. Fröbert, Instantaneous wave-free ratio versus fractional flow reserve to guide pci. *New Engl. J. Med.* **376** (2017), No. 19, 1813–1823.

10. K. L. Gould, R. L. Kirkeeide, and M. Buchi, Coronary flow reserve as a physiologic measure of stenosis severity. *J. Amer. Coll. Cardiol.* **15** (1990), No. 2, 459–474.

11. L. Grady, Fast, quality, segmentation of large volumes – isoperimetric distance trees. In: *Computer Vision – ECCV 2006*. Springer, Berlin–Heidelberg, 2006, pp. 449–462.

12. J. Hashemi, B. Patel, Y. S. Chatzizisis, and G. S. Kassab, Real time reduced order model for angiography fractional flow reserve. *Comput. Meth. Programs Biomed.* **216** (2022) 106674.

13. A. R. Ihdayhid, T. Sakaguchi, J. J. Linde, M. H. Sørgaard, K. F. Kofoed, Y. Fujisawa, J. Hislop-Jambrich, N. Nerlekar, J. D. Cameron, R. K. Munnur, M. Crosset, D. T. L. Wong, S. K. Seneviratne, and B. S. Ko, Performance of computed tomography-derived fractional flow reserve using reduced-order modelling and static computed tomography stress myocardial perfusion imaging for detection of haemodynamically significant coronary stenosis. *Eur. Heart J. Cardiovas. Imaging* **19** (2018), No. 11, 1234–1243.

14. G. Lavinia, H. Jonathan, R. G. Thomas, and N. Curzen, Fractional flow reserve derived from coronary computed tomography: Where are we now and where are we heading? *Future Cardiology* **17** (2020), No. 6, 723–741.

15. E. W. Lo, L. J. Menezes, and R. Torii, On outflow boundary conditions for CT-based computation of FFR: Examination using PET images. *Med. Eng. Phys.* **76** (2020), 79–87.

16. M. McCormick, X. Liu, J. Jomier, C. Marion, and L. Ibanez, ITK: enabling reproducible research and open science. *Frontiers in Neuroinformatics* **8** (2014).

17. P. D. Morris, F. N. van de Vosse, P. V. Lawford, D. R. Hose, and J. P. Gunn, "Virtual" (computed) fractional flow reserve. *JACC: Cardiovascular Interventions* **8** (2015), No. 8, 1009–1017.

18. H. Omori, M. Hara, Y. Sobue, Y. Kawase, T. Mizukami, T. Tanigaki, T. Hirata, H. Ota, M. Okubo, A. Hirakawa, T. Suzuki, T. Kondo, J. Leipsic, B. L. Nørgaard, and H. Matsuo, Determination of the optimal measurement point for fractional flow reserve derived from CT angiography using pressure wire assessment as reference. *Amer. J. Roentgenology* **216** (2020), No. 6, 1492–1499.

19. C. Pudney, Distance-ordered homotopic thinning: A skeletonization algorithm for 3D digital images. *Comput. Vis. Image Underst.* **72** (1998), No. 3, 404–413.

20. A. Ruiz-Muñoz, F. Valente, L. Dux-Santoy, A. Guala, G. Teixidó-Turà, L. Galián-Gay, L. Gutiérrez, R. Fernández-Galera, G. Casas, T. González-Alujas, I. Ferreira-González, A. Evangelista, and J. Rodr´iguez-Palomares, Diagnostic value of quantitative parameters for myocardial perfusion assessment in patients with suspected coronary artery disease by single- and dual-energy computed tomography myocardial perfusion imaging. *IJC Heart & Vasculature* **32** (2021) 100721.

21. S. Simakov, T. Gamilov, F. Liang, and P. Kopylov, Computational analysis of haemodynamic indices in synthetic atherosclerotic coronary networks. *Mathematics* **9** (2021), No. 18, 2221.

22. S. S. Simakov, T. M. Gamilov, F. Liang, D. G. Gognieva, M. K. Gappoeva, and P. Y. Kopylov, Numerical evaluation of the effectiveness of coronary revascularization. *Russ. J. Numer. Anal. Math. Modelling* **36** (2021), No. 5, 303–312.

23. S. S. Simakov, T. M. Gamilov, A. A. Danilov, F. Liang, P. S. Chomakhidze, M. K. Gappoeva, A. A. Rebrova, and P. Y. Kopylov, Personalized computational estimation of relative change in coronary blood flow after percutaneous coronary intervention in short-term and long-term perspectives. *Russ. J. Numer. Anal. Math. Modelling* **37** (2022), No. 5, 279–291.

24. S. S. Simakov, T. M. Gamilov, F. Liang, P. S. Chomakhidze, and P. Y. Kopylov, Validation of boundary conditions for coronary circulation model based on a lumped parameter approach. *Russ. J. Numer. Anal. Math. Modelling* **38** (2023), No. 3, 161–172.

25. A. Suyundukova, V. Demkin, A. Mochula, M. Gulya, A. Maltseva, and K. Zavadovsky, State of the art mathematical methods of the coronary blood flow modelling: background and clinical

value. *Kardiologiia* **63** (2023), No. 3, 77–84 (in Russian).

26. C. A. Taylor, T. A. Fonte, and J. K. Min, Computational fluid dynamics applied to cardiac computed tomography for noninvasive quantification of fractional flow reserve. *J. Amer. Coll. Cardiol.* **61** (2013), No. 22, 2233–2241.

27. Y. Vassilevski, T. Gamilov, A. Danilov, G. Kopytov, and S. Simakov, A web-based non-invasive estimation of fractional flow reserve (FFR): Models, algorithms, and application in diagnostics. In: *Trends in Biomathematics: Modeling Epidemiological, Neuronal, and Social Dynamics*. Springer Nature, Switzerland, 2023, pp. 305–316.

28. Y. Vassilevski, M. Olshanskii, S. Simakov, A. Kolobov, and A. Danilov, *Personalized Computational Hemodynamics*. Elsevier, 2020.